

- al., *ibid.* **147**, 2493 (1991); S. Jalkanen et al., *Eur. J. Immunol.* **16**, 1195 (1986).
3. R. Arch et al., *Science* **257**, 682 (1992).
 4. S. Seiter et al., *J. Exp. Med.* **177**, 443 (1993); U. G. Ånther et al., *Cell* **65**, 13 (1991).
 5. M. Culty et al., *J. Cell Biol.* **111**, 2765 (1990).
 6. R. P. Singh et al., *J. Exp. Med.* **171**, 1931 (1990).
 7. R. Patarca, R. A. Saavedra, H. Cantor, *Crit. Rev. Immunol.* **13**, 225 (1993); G. A. Rodan, *Ann. N.Y. Acad. Sci.* **760**, 1 (1995).
 8. D. T. Denhardt and X. Guo, *FASEB J.* **7**, 1475 (1993).
 9. D. R. Senger, C. A. Perruzzi, A. Papadopoulos, *Anticancer Res.* **9**, 1291 (1989); A. M. Craig et al., *Int. J. Cancer* **46**, 133 (1990); A. F. Chambers et al., *Anticancer Res.* **12**, 43 (1992); E. I. Behrend et al., *Cancer Res.* **54**, 832 (1994).
 10. M. D. McKee et al., *Anat. Rec.* **228**, 77 (1990); M. D. McKee, M. J. Glimcher, A. Nanci, *ibid.* **234**, 479 (1992).
 11. R. Patarca et al., *J. Exp. Med.* **170**, 145 (1989).
 12. S. Ashkar et al., *Biochem. Biophys. Res. Commun.* **191**, 126 (1993).
 13. A. Oldberg, A. Franzen, D. Heinegard, *Proc. Natl. Acad. Sci. U.S.A.* **83**, 8819 (1986); A. Oldberg et al., *J. Biol. Chem.* **263**, 19433 (1988); M. Sato et al., *J. Cell Biol.* **111**, 1713 (1990); L. Liaw et al., *J. Clin. Invest.* **95**, 713 (1995).
 14. S. van Dijk et al., *J. Bone Miner. Res.* **8**, 1499 (1993).
 15. K8 cells are differentiated osteosarcoma cells that display high metastatic activity and secrete large amounts of Opn [O. Aresu et al., *Invasion Metastasis* **11**, 2 (1991); J. Schmidt et al., *Differentiation* **39**, 151 (1988)], which is O-glycosylated, not N-glycosylated, contains eight phosphates per mole of protein, and does not express detectable hyaluronate. Osteopontin purified from K8 supernatants by antibody-dependent affinity chromatography was homogenous according to NH₂-terminal sequence analysis.
 16. Two and a half picomoles of ³²P-labeled immunofluorescence-purified Opn from K8 cells was added to 1 × 10⁶ WEHI-3B cells (about half the saturating concentration), incubated at room temperature in the presence or absence of antibody to CD44 (anti-CD44) or control antibody [mAb Pgp-1, clone IM7 from Pharmingen; mAb KM 81, clone TIB241 from the American Type Culture Collection (ATCC); and rat IgG from Sigma] at 3 μg or a 200-fold excess of unlabeled Opn in 250 μl before bound and free fractions were separated by centrifugation as described (6) in four separate experiments. Similar results were obtained for binding of recombinant phosphorylated Opn to K8 cells.
 17. CD44 was expressed in the murine embryonic cell line A31 after amplification of cDNA from K8 cells with 5'-CAGAATTCCTCGATCTCTGGTAAGGAG-3' and 5'-TAGGATCCTGCCTCAACTGTGCACTCA-3' primers, resulting in a single species of cDNA containing exons 7v through 10v according to PCR and sequencing analysis. This cDNA was cloned into the Bam HI-Eco RI sites of the eukaryotic expression vector pcDNA III/neo (Invitrogen, San Diego CA), which contains enhancer-promoter sequences from the early gene of human cytomegalovirus, the SV40 polyadenylation-transcription termination signal, and the neomycin resistance gene for selection. CD44 clones were transfected into the A31 mouse embryonic fibroblast cell line by electroporation and selection according to G418 resistance and adherence to HA.
 18. The AF3.G7 hybridoma, generated by fusing cow insulin-immune C57BL/6 lymph node cells with the BW5147 thymoma line, responds to cow insulin according to interleukin-2 production [D. G. Spinella et al., *J. Immunol.* **138**, 3991 (1987)] and expresses CD44 on its cell surface as judged by flow cytometry analysis with Pgp-1 antibody (clone IM7, Pharmingen). AF3.G7 cells were lysed in 0.1% Triton X-100 buffer containing 25 mM potassium phosphate, pH 7.4, 4 mM EDTA, 10 mM sodium chloride, 5 mM magnesium chloride, 10 mM iodoacetamide, 0.025% (w/v) sodium azide, 0.2 U/ml of aprotinin, 20 mg/ml of pepstatin A, 1 mM phenylmethylsulfonyl fluoride, and 1 mM sodium orthovanadate, and centrifuged at 100,000g before the supernatant was filtered and loaded onto the indicated affinity resins overnight. After extensive washing, the bound protein was eluted with 3 M NaSCN and salt was removed in Centricon filter units and Excelsolve GF-5 detergent removal columns (Pierce) followed by concentration in Microsep 10K filters (Filtron).
 19. M. A. Moses, J. Sudhalter, R. Langer, *Science* **248**, 1408 (1990).
 20. L. Liaw et al., *Circ. Res.* **74**, 214 (1994).
 21. J. Lesley, R. Schulte, R. Hyman, *Exp. Cell Res.* **187**, 224 (1990).
 22. F. P. Reinholt, K. Hultenby, A. Oldberg, D. Heinegard, *Proc. Natl. Acad. Sci. U.S.A.* **87**, 4473 (1990).
 23. T. L. Yue et al., *Exp. Cell Res.* **214**, 459 (1994).
 24. G. F. Weber, S. Abromson-Leeman, H. Cantor, *Immunology* **2**, 363 (1995).
 25. Cells (0.2 × 10⁶) were incubated with biotinylated ligand in 150 μl of calcium- and magnesium-free phosphate-buffered saline (PBS) for 30 min at 37°C followed by fixation in 1% paraformaldehyde for 10 min on ice. After resuspension in calcium- and magnesium-free PBS, phycoerythrin-streptavidin was added at 1:100 dilution for 20 min on ice, and cells were washed and analyzed with a Coulter Profile flow cytometer.
 26. Plates (96 well) were coated with either 10 μg/ml of Opn, 10 μg/ml of fibronectin, or 100 μg/ml of HA for 18 hours at 4°C followed by blocking with 1 mg/ml of BSA (bovine serum albumin) for 2 hours at room temperature. One thousand cells per well were incubated at 37°C in calcium-free and magnesium-free PBS containing 100 μg/ml of BSA. After 30 min the cells were fixed in 4% paraformaldehyde in PBS and stained with toluidine blue. Attachment was assessed by counting the total number of cells per well. Soluble inhibitors were added at the following concentrations: GRGDS peptide, 1 mM; Opn, 500 μg/ml; hyaluronic acid (HA), 1 mg/ml.
 27. A31.MLV or A31.C1 cells (1 × 10⁴ cells/well) in calcium- and magnesium-free PBS were incubated with either 100 μg of HA or 50 μg of Opn for 15 min at 4°C. In experiments with blocking antibody, cells were incubated with CD44 antibody KM 81 (TIB 241 supernatant; 1:20 dilution) for 15 min before addition of ligand. Cells were scored positive when more than 50% of the cells were in aggregates of four or more cells.
 28. J. A. Wass et al., *J. Natl. Cancer Inst.* **66**, 927 (1981).
 29. Surfaces of polycarbonate filters (pore size, 8 μm) were coated with 5 μg of fibronectin before 1 × 10⁵ cells were added in 500 μl to the upper chamber and incubated at 37°C in the presence or absence of chemotactic agents in the lower chamber. After 4 hours, the membranes were fixed in methanol and stained with hematoxylin + toluidine blue. Responding cells on the lower surface of the filter were counted microscopically and evaluated in triplicates.
 30. S. Ashkar et al., *Ann. N.Y. Acad. Sci.* **760**, 296 (1995).
 31. This study was supported in part by NIH research grants AI12184 and AI13600 to H.C.; NIH grant PO1 AR34078 and a grant from the Peabody Foundation to M.J.G.; and a Barr Program Small Grant to G.F.W. J. Schmidt and L. Gerstenfeld provided the K8 osteosarcoma cell line. The authors are grateful to L. Glimcher, C. Rudd, and G. Dranoff for critical reading of the manuscript, to W. Fu for expert technical assistance, and to A. Angel for assistance in the preparation of the manuscript.

8 September 1995; accepted 4 December 1995

Activation by Attention of the Human Reticular Formation and Thalamic Intralaminar Nuclei

Shigeo Kinomura, Jonas Larsson, Balázs Gulyás, Per E. Roland*

It has been known for over 45 years that electrical stimulation of the midbrain reticular formation and of the thalamic intralaminar nuclei of the brain alerts animals. However, lesions of these sectors fail to impair arousal and vigilance in some cases, making the role of the ascending activating reticular system controversial. Here, a positron emission tomographic study showed activation of the midbrain reticular formation and of thalamic intralaminar nuclei when human participants went from a relaxed awake state to an attention-demanding reaction-time task. These results confirm the role of these areas of the brain and brainstem in arousal and vigilance.

Electrical stimulation of the midbrain reticular formation (MRF), an evolutionarily ancient part of the mammalian brainstem (Fig. 1), produces desynchronization in electroencephalograms (EEGs) and awakens and arouses animals (1). Electrocoagulation of this area induces a comatose state and the absence of EEG desynchronization and behavioral arousal to sensory stimuli (2). These observations led to the concept of an ascending reticular activating system and were corroborated by anatomical and electrophysiological studies showing that the MRF sends efferents to the intralaminar

thalamic nuclei. These studies also showed that the MRF and intralaminar nuclei, when stimulated artificially or by sensory stimuli, in concert evoked EEG desynchronization and behavioral arousal and woke up the experimental animals (3, 4).

However, it has been difficult to reproduce the electrocoagulation findings by more refined methods that destroy only the neuronal perikarya of the MRF and not the traversing axons (5). Whereas recordings from MRF neurons have documented the involvement of this part of the brainstem in the transition between sleep and the awake state (6, 7), direct evidence that the MRF and intralaminar nuclei are tonically engaged in maintaining a state of high vigilance and attention has been lacking. We therefore measured the regional cerebral

Division of Human Brain Research, Department of Neuroscience, Karolinska Institute, S-171 77 Stockholm, Sweden.

*To whom correspondence should be addressed.

blood flow (rCBF) in 10 normal volunteers at rest and when they were engaged in two difficult and attention-demanding somatosensory and visual reaction-time tasks. Our hypothesis was that transition from an awake relaxed state into a state of high vigilance and attention that occurs during reaction-time tasks would increase the synaptic activity of the neurons in the MRF and intralaminar thalamic nuclei and increase the rCBF in these areas (8). Although the MRF cannot always be localized in positron emission tomography (PET) scans, the midbrain tegmentum and the intralaminar thalamic nuclei can be localized stereotaxically and in high-resolution magnetic resonance tomography of the brain (9).

The rCBF was measured by PET (9) in 10 healthy volunteers (10), 9 right-handed

and 1 ambidextrous (11), under three conditions: during rest (12), during a visual reaction-time (vis-RT) task, and during a somatosensory reaction-time (som-RT) task. During rest, the participants were supine with their eyes closed and held a response key in their right hand. In the vis-RT task, the participants fixated on a yellow circle on a monitor, which at random time intervals suddenly increased in luminance. In response, they pressed the key with their right thumb as soon as possible after the increase in luminance (13). During the som-RT, the participants also had their eyes open and fixated on the yellow circle. Their task here was to press the key as soon as possible after feeling the sudden indentation of a stylus on the right index finger (14). Thus, the differences between the rest condition and the reaction-time

conditions were the open eyes, the fixation on the yellow circle, and the increased vigilance and attention associated with the fast responses, the stimuli, and the motor responses (15).

Compared to the rest condition, the vis-RT task and the som-RT task both increased the rCBF markedly in the midbrain tegmentum and the left intralaminar region of the thalamus (Fig. 1). The activation of the midbrain extended for 17 mm throughout the right midbrain tegmentum containing the MRF (16) (Fig. 1). The thalamic activation extended from 8 to 11 mm on the left of the midline and from -16 to -22 mm posterior to the intercommissural plane (Table 1). This corresponds to the centro-median and centralis lateralis nuclei of the intralaminar group (17). Although the increases of rCBF were statistically sig-

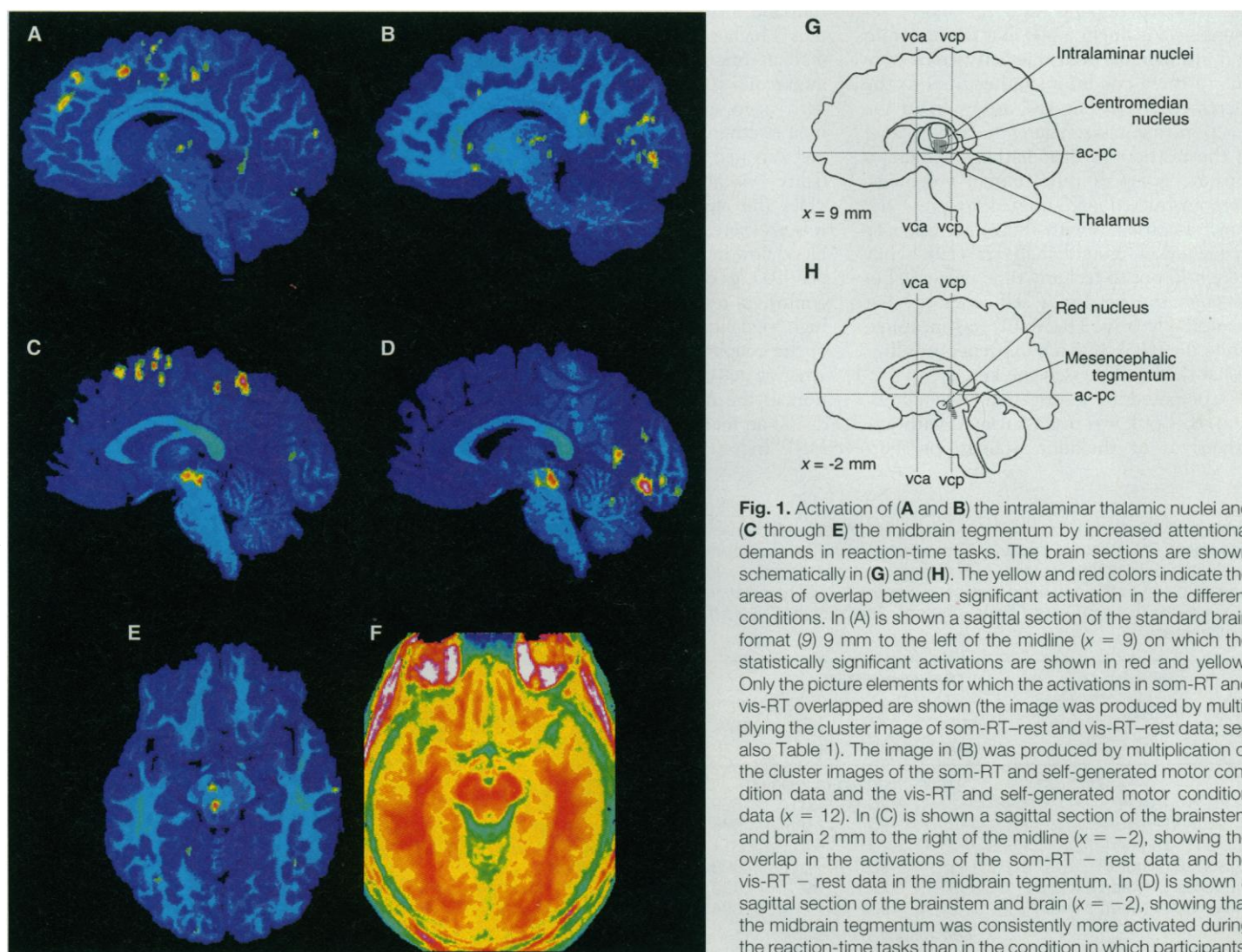


Fig. 1. Activation of (A and B) the intralaminar thalamic nuclei and (C through E) the midbrain tegmentum by increased attentional demands in reaction-time tasks. The brain sections are shown schematically in (G) and (H). The yellow and red colors indicate the areas of overlap between significant activation in the different conditions. In (A) is shown a sagittal section of the standard brain format (9) 9 mm to the left of the midline ($x = 9$) on which the statistically significant activations are shown in red and yellow. Only the picture elements for which the activations in som-RT and vis-RT overlapped are shown (the image was produced by multiplying the cluster image of som-RT-rest and vis-RT-rest data; see also Table 1). The image in (B) was produced by multiplication of the cluster images of the som-RT and self-generated motor condition data and the vis-RT and self-generated motor condition data ($x = 12$). In (C) is shown a sagittal section of the brainstem and brain 2 mm to the right of the midline ($x = -2$), showing the overlap in the activations of the som-RT - rest data and the vis-RT - rest data in the midbrain tegmentum. In (D) is shown a sagittal section of the brainstem and brain ($x = -2$), showing that the midbrain tegmentum was consistently more activated during the reaction-time tasks than in the condition in which participants, with their eyes open, pressed the response button. The image was produced by multiplication of the cluster images of the som-RT - motor condition data and the vis-RT - motor condition data. In (E) is a horizontal section 9 mm below the intercommissural plane ($z = -9$), showing the overlap in the activations of the som-RT - rest data and the vis-RT - rest data. (F) Same section as in (E), but showing the mean image produced from the anatomically standardized set of the 10 individual nuclear magnetic resonance images of the participants in the reaction-time tasks. This image reveals the accuracy of the anatomical standardizations. Schematic sections of the standard brain of *Human Brain Mapping* (23) are in (G) and (H), showing (G) the positions of the intralaminar nuclei and (H) the midbrain tegmentum (24).

was produced by multiplication of the cluster images of the som-RT - motor condition data and the vis-RT - motor condition data. In (E) is a horizontal section 9 mm below the intercommissural plane ($z = -9$), showing the overlap in the activations of the som-RT - rest data and the vis-RT - rest data. (F) Same section as in (E), but showing the mean image produced from the anatomically standardized set of the 10 individual nuclear magnetic resonance images of the participants in the reaction-time tasks. This image reveals the accuracy of the anatomical standardizations. Schematic sections of the standard brain of *Human Brain Mapping* (23) are in (G) and (H), showing (G) the positions of the intralaminar nuclei and (H) the midbrain tegmentum (24).

nificant in the right midbrain tegmentum and left intralaminar nuclei of the thalamus only, there were no significant differences in rCBF between the right and left homologs of these structures (18). There were no other rCBF increases in the brainstem, but there was one increase in the left ventral and lateral part of the thalamus in the som-RT task. The magnitude of the increases of rCBF in the midbrain tegmentum and thalamic intralaminar nuclei (Table 1) made it highly unlikely that the activation of the right midbrain tegmentum and left intralaminar nuclei of the thalamus were significant because of the moderate general increase of rCBF accompanying the vis-RT and som-RT tasks (15).

Because there were behavioral differences between the rest condition and the reaction-time conditions—that is, opening of the eyes, fixating on the yellow circle, the intention to respond, and the motor response—one might argue that the midbrain and intralaminar thalamic activations were due to these conditions rather than to the increase in vigilance and attention in the reaction-time tasks. Therefore, and because of the restrictions of radiation exposure, a separate group of nine normal volunteers were instructed and trained to press the same response key with an average response frequency of around 0.33 Hz (19). They were told not to feel any time pressure, but to press the key in a self-generated but comfortable way. The rCBF was measured while they looked at a homogeneous yellow visual field and pressed the key.

Compared to a rest reference condition, this task was not associated with any brainstem or thalamic activations. Fur-

thermore, when the image of the mean rCBF during the self-generated key presses was subtracted from those of the reaction-time tasks, the right midbrain tegmentum and left intralaminar thalamic nuclei regions were significantly more activated in the som-RT and the vis-RT tasks ($P < 0.01$ in both cases) (9) (Fig. 1). This made it unlikely that the mesencephalic tegmental and thalamic intralaminar activations were associated with the opening of the eyes or with the motor preparation or the actual key press. Also, it is unlikely that sensory stimulation such as that experienced in situations of moderate sensory attention with no time pressure would markedly increase rCBF in the midbrain tegmentum and intralaminar thalamic nuclei. This interpretation is also supported by other studies (20).

Thus, the rCBF in the midbrain tegmentum and intralaminar domain of the thalamus is higher during high vigilance and general attention than when participants are awake and resting or when they are awake with open eyes, performing self-generated motor activity. Furthermore, these structures are activated irrespective of the sensory modality (visual or somatosensory) that provides the alerting signal. Their activation was associated with a diffuse increase of the blood flow in the cerebral cortex of 3 to 4 ml per 100 g of tissue per minute (ml/100 g/min), a result expected in situations of high vigilance and attention (21). Because of the coupling between rCBF and regional synaptic activity, we submit that the activation of the mesencephalic tegmentum was due to an increase in synaptic activity of the MRF. Indeed, in cats MRF neurons directly

activate thalamic intralaminar neurons with identified cortical projections, and the thalamic neurons increase their firing during alertness (4, 7). Because our participants were awake during the control condition, the mesencephalic tegmental and thalamic intralaminar nuclei thus might control not only the transition from sleep to an alert state, but also the transition from relaxed wakefulness to high general attention and the maintenance of general attention.

REFERENCES AND NOTES

1. G. Moruzzi and H. W. Magoun, *Electroencephalogr. Clin. Neurophysiol.* **1**, 455 (1949).
2. D. B. Lindsley, L. H. Schreiner, W. B. Knowles, H. W. Magoun, *ibid.* **2**, 483 (1950); J. D. French and H. W. Magoun, *Arch. Neurol. Psychiatry* **68**, 591 (1952); M. E. Scheibel and A. B. Scheibel, in *Reticular Formation of the Brain*, H. H. Jasper, L. D. Proctor, R. S. Knighton, W. C. Noshay, R. T. Costello, Eds. (Little Brown, Boston, 1958), pp. 31–55.
3. M. Steriade, A. Parent, N. Ropert, A. Kitsikis, *Brain Res.* **238**, 13 (1982); B. Hu, M. Steriade, M. Deschênes, *Neuroscience* **31**, 1 (1989).
4. M. Steriade and L. L. Glenn, *J. Neurophysiol.* **48**, 352 (1982).
5. M. Sallanon, K. Sakai, C. Buda, M. Puymartin, M. Jouvret, *Arch. Ital. Biol.* **126**, 87 (1988); A. Kitsikis and M. Steriade, *Behav. Brain Res.* **3**, 361 (1981); H. H. Webster and B. E. Jones, *Brain Res.* **458**, 285 (1988); M. Denoyer, M. Sallanon, C. Buda, K. Kitamura, M. Jouvret, *ibid.* **539**, 287 (1991).
6. M. Steriade, G. Oakson, N. Ropert, *Exp. Brain Res.* **46**, 37 (1982).
7. L. L. Glenn and M. Steriade, *J. Neurosci.* **2**, 1387 (1982).
8. L. Sokoloff *et al.*, *J. Neurochem.* **28**, 897 (1977); J. Greenberg, P. Hand, A. Sylvestro, M. Reivich, *Acta Neurol. Scand.* **60** (suppl. 72), 12 (1979).
9. All participants underwent magnetic resonance tomography and PET while equipped with the same stereotaxic helmet [M. Bergström *et al.*, *J. Comput. Assisted Tomogr.* **5**, 136 (1981)]. The magnetic resonance tomograms were SPGR (radiofrequency spoiled gradient echo) three-dimensional sequences obtained with a 1.5 T General Electric Signa scanner, where TE (echo time) = 5 ms, TR (repetition time) = 21 ms, θ (flip angle) = 50°, and FOV (field of view) = 256 mm. The rCBF was measured with an eight-ring, 15-slice PET camera (PC2048-15B, Scanditronix) with an in-plane spatial resolution of 4.5 mm and an interslice distance of 6.5 mm. Seventy microliters of ^{15}O -butanol was injected intravenously as a bolus. The arterial input function was continuously monitored, and the rCBF was calculated (ml/100 g/min) on the data from 0 to 80 s as described (22). The images were reconstructed with a 4-mm Hanning filter. Correction for differences in rCBF due to differences in alveolar CO_2 pressure was done before test minus control subtractions to the level of alveolar CO_2 pressure of the control. Subsequently, the rCBF of the control condition was subtracted from that of the test condition. The resulting subtraction images were anatomically standardized (23), and descriptive Student's *t* pictures were calculated (22). The criteria for accepting rCBF changes in adjacent clustered voxels as activations were set so that there was an average probability of less than 0.005 of finding one false-positive cluster in the three-dimensional space representing the brainstem and thalamus (22).
10. All participants reported no previous neurological, psychological, or medical problems and all had normal magnetic resonance tomograms of the skull and brain.
11. Handedness was assessed by a Swedish version of the technique described in R. C. Oldfield, *Neuropsychologia* **9**, 97 (1971). The laterality coefficients ranged between 65 and 90 with a mean of $73.3 \pm$

Table 1. Activation of brainstem and thalamus. Abbreviations are as follows: motor, self-generated movement; CG, center of gravity; M/L, medial/lateral (negative value indicates right side, positive value left side of the brain and brainstem); A/P, anterior/posterior (negative value indicates position anterior to the tangent plane to the anterior commissure); and S/I, superior/inferior (negative value indicates position inferior to the biocommissural plane). The coordinates of the CG are those of *Human Brain Mapping* (23) in millimeters.

Task	Coordinates of CG			Volume (mm ³)	Δ rCBF mean \pm SEM (ml/100 g/min)	Mean <i>t</i> value
	M/L (x)	A/P (y)	S/I (z)			
<i>Right midbrain-tegmentum</i>						
a. Vis-RT–rest	–2	–25	–8	609	17.4 \pm 6.5	3.0
b. Som-RT–rest	–3	–25	–9	578	16.5 \pm 6.6	2.9
c. Vis-RT–motor	–2	–23	–7	611	22.5 \pm 7.6	2.9
d. Som-RT–motor	–1	–23	–8	693	20.9 \pm 7.2	2.8
Overlap between a and b	–3	–22	–9	430		
Overlap between c and d	–2	–22	–7	384		
<i>Left intralaminar thalamic nuclei</i>						
a. Vis-RT–rest	8	–21	5	300	15.9 \pm 5.3	2.9
b. Som-RT–rest	8	–18	3	312	16.5 \pm 5.8	2.4
c. Vis-RT–motor	9	–22	3	333	15.5 \pm 7.8	2.3
d. Som-RT–motor	8	–21	2	302	13.8 \pm 7.8	2.3
Overlap between a and b	8	–20	6	59		
Overlap between c and d	8	–22	3	152		

8.5 (SD) for the right-handers and -10 for the ambidextrous participant.

12. Rest was as defined [P. E. Roland and B. Larsen, *Arch. Neurol.* **33**, 551 (1976)]. The arterial partial pressure of CO₂ and O₂ was measured repetitively, and the EEG and electrooculogram (EOG) were recorded continuously. None of the participants broke their fixated gazes, and the EOG showed only eye blinks with an average frequency of 0.2 ± 0.1 Hz (mean ± SD). The background illumination was 0.27 cd/m² during all conditions.
13. The visual stimulus for fixation was a 3° visual angle yellow monochrome circle 0.8 cd/m² on a monitor. At random intervals ranging from 1000 to 3000 ms, the luminance of the circle suddenly increased to 14.5 cd/m² for 1000 ms.
14. Experiment participants during all conditions rested the pad of the right index finger on a polyvinyl plate having an 11-mm-diameter hole through which a 2-mm stylus driven by a solenoid could protrude. The stylus did not touch the skin in the interstimulus intervals. The interstimulus intervals ranged from 1000 to 3000 ms in a random manner. In the somatosensory task, the stylus indented the pulp of the index finger by 2.8 mm for 1000 ms.
15. The visual reaction time was 315 ± 39 ms (mean ± SD); the somatosensory reaction time was 288 ± 29 ms. The global blood flow of the brain increased from 46.1 ± 5.3 ml/100 g/min at rest to 49.5 ± 4.6 ml/100 g/min and 50.5 ± 4.9 ml/100 g/min in the vis-RT and som-RT tasks, respectively. The percentage α-blockade in the EEG was 80.1 ± 17.2 (mean ± SD) during rest and 80.1 ± 20.1 during the som-RT task but increased to 90.7 ± 8.2 during the vis-RT task (*P* < 0.01; *t* test). Heart rate did not change significantly [62.0 ± 6.0 beats/min (rest), 62.8 ± 6.6 beats/min (vis-RT), and 63.2 ± 6.7 beats/min (som-RT)]; neither did the arterial CO₂ pressure [5.59 ± 0.23 kPa (rest), 5.56 ± 0.23 kPa (vis-RT), and 5.62 ± 0.33 kPa (som-RT)].
16. The accuracy (SEM) of localizing structures in the upper brainstem in PET and magnetic resonance images was <0.35 mm. The center of gravity of the right red nucleus was determined in the brainstem in each participant (23). In the anatomically standardized format, the mean coordinates ± SEM for the 10 participants were *x* (medial-lateral), 5.16 ± 0.19 mm; *y* (anterior-posterior), 18.90 ± 0.31 mm; and *z* (superior-inferior), 6.86 ± 0.19 mm.
17. G. Schaltenbrand and P. Bailey, *Einführung in die Stereo-taktischen Operationen mit einem Atlas des menschlichen Gehirns* (Thieme Verlag, Stuttgart, 1959).
18. The rCBFs in the right and left midbrain tegmentum were 54.9 ± 4.9 ml/100 g/min and 53.5 ± 4.9 ml/100 g/min, respectively, for the som-RT (mean ± SEM); for the vis-RT task, the corresponding values were 54.7 ± 5.3 and 53.9 ± 5.6 ml/100 g/min, respectively. For the right and left intralaminar nuclei of the thalamus, the rCBFs were 64.5 ± 4.3 ml/100 g/min and 69.7 ± 6.3 ml/100 g/min, respectively, for the som-RT, and 74.9 ± 4.4 ml/100 g/min and 68.6 ± 6.5 ml/100 g/min, respectively, for the vis-RT task. For comparison, a ROI (region of interest) symmetrical to the activated part was drawn.
19. The experiment participants were nine normal male volunteers aged 23 to 29 years, eight of whom were right-handed and one of whom was left-handed. In the task, they were trained for 10 min to produce a rate acceptably close to the stipulated 0.33 Hz. The luminance of the homogenous yellow light on the screen was 4.2 cd/m². The color coordinates were *x* = 0.51 and *y* = 0.426 (Commission International d'Éclairage). The procedures and PET measurements were identical to those made in the reaction-time group. The global rCBF was 46.6 ± 5.4 ml/100 g/min. The α-blockade was 79.3 ± 16.5%, the frequencies of eye blinks 0.3 ± 0.1 Hz, and the arterial CO₂ pressure 5.56 ± 0.24 kPa, all of which were similar to the values obtained in the rest and RT conditions. Specifically, there were no differences in the frequency of thumb movements in the RT conditions and the self-generated movement condition, values for which were as follows: 0.35 ± 0.01 Hz (vis-RT), 0.31 ± 0.02 Hz (som-RT), and 0.29 ± 0.06 Hz (self-generated thumb movements). Other proce-

dures were as described (9).

20. J. Decety, R. Kawashima, B. Gulyás, P. E. Roland, *NeuroReport* **3**, 761 (1992); B. T. O'Sullivan, P. E. Roland, R. Kawashima, *Eur. J. Neurosci.* **6**, 137 (1994); R. Kawashima, B. T. O'Sullivan, P. E. Roland, *Cerebr. Cortex* **2**, 111 (1995).
21. S. S. Kety, *Am. J. Med.* **8**, 205 (1950); D. Ingvar *et al.*, *Arch. Neurol.* **11**, 13 (1964); P. E. Roland, L. Eriksson, S. Stone-Elander, L. Widén, *J. Neurosci.* **7**, 2373 (1987); P. E. Roland, *Brain Activation* (Wiley, New York, 1993).
22. P. E. Roland *et al.*, *Human Brain Mapping* **1**, 3 (1993).

23. P. E. Roland *et al.*, *ibid.* **1**, 173 (1994).
24. The vca plane, which is tangent to the anterior commissure, defines the zero coordinate in the the anterior-posterior axis (Table 1). The vcp plane is vertical tangent to the posterior commissure. The ac-pc (commissural) plane defines the zero coordinate in the superior-inferior axis.
25. Supported by the Human Capital and Mobility Programme of the European Commission and the Swedish Medical Research Council. We thank J. Pedersen and W. Pulka for technical assistance.

6 June 1995; accepted 21 November 1995

Altered Reactivity of Superoxide Dismutase in Familial Amyotrophic Lateral Sclerosis

Martina Wiedau-Pazos,* Joy J. Goto,* Shahrooz Rabizadeh, Edith B. Gralla, James A. Roe, Michael K. Lee, Joan S. Valentine,† Dale E. Bredesen†

A subset of individuals with familial amyotrophic lateral sclerosis (FALS) possesses dominantly inherited mutations in the gene that encodes copper-zinc superoxide dismutase (CuZnSOD). A4V and G93A, two of the mutant enzymes associated with FALS, were shown to catalyze the oxidation of a model substrate (spin trap 5,5'-dimethyl-1-pyrroline *N*-oxide) by hydrogen peroxide at a higher rate than that seen with the wild-type enzyme. Catalysis of this reaction by A4V and G93A was more sensitive to inhibition by the copper chelators diethyldithiocarbamate and penicillamine than was catalysis by wild-type CuZnSOD. The same two chelators reversed the apoptosis-inducing effect of mutant enzymes expressed in a neural cell line. These results suggest that oxidative reactions catalyzed by mutant CuZnSOD enzymes initiate the neuro-pathologic changes in FALS.

Amyotrophic lateral sclerosis (ALS), or Lou Gehrig's disease, is a motor neuron degenerative disease that affects approximately 1 person in 10,000. About 10 to 15% of cases are familial (1), and 20 to 25% of familial ALS (FALS) cases are associated with dominantly inherited mutations in *SOD1*, the gene that encodes human CuZnSOD (2). Initial studies of the FALS-associated CuZnSOD mutants appeared to demonstrate reduced enzymatic activity (3). However, subsequent studies with transgenic mouse (4) and cell culture (5) models of FALS indicated a dominant, gain-of-function effect of the FALS-associated CuZnSOD mutants. Moreover, yeast *sod1* null mutants were rescued as efficiently by

FALS-associated mutant human CuZnSOD as by the wild-type (WT) human enzyme, which indicated extensive activity of the mutant proteins (5). Although these observations supported a gain-of-function effect of the mutants, the nature of the function gained has remained undetermined (1).

In addition to its activity as a SOD (6), CuZnSOD catalyzes oxidation of substrates by hydrogen peroxide (H₂O₂) at rates competitive with its own oxidative inactivation by the same reagent (7, 8). A convenient substrate used to study this type of reaction is the spin trap 5,5'-dimethyl-1-pyrroline *N*-oxide (DMPO), which reacts with H₂O₂ to give its electron paramagnetic resonance (EPR)-detectable hydroxyl adduct, DMPO-OH, in a reaction catalyzed by WT CuZnSOD (9). We hypothesized that the FALS-associated mutant CuZnSODs might enhance similar oxidative reactions of substrates with H₂O₂ because the locations of the FALS-associated mutations in this enzyme suggest the possibility of increased openness of the three-dimensional structures (3), which could conceivably allow greater access of substrates to the active site. In addition, in a neuronal cell culture model of FALS, mutant human CuZnSODs [Ala⁴ → Val (A4V) and Gly³⁷ → Arg (G37R)] increased apoptosis, whereas the

M. Wiedau-Pazos, J. J. Goto, E. B. Gralla, J. S. Valentine, Department of Chemistry and Biochemistry, University of California, Los Angeles, CA 90095, USA.

S. Rabizadeh, Interdepartmental Program for Neuroscience, University of California, Los Angeles, CA 90095, USA, and Program on Aging, La Jolla Cancer Research Foundation, La Jolla, CA 92037, USA.

J. A. Roe, Department of Chemistry and Biochemistry, Loyola Marymount University, Los Angeles, CA 90045, USA.

M. K. Lee, Department of Pathology, Johns Hopkins University School of Medicine, Baltimore, MD 21218, USA. D. E. Bredesen, Program on Aging, La Jolla Cancer Research Foundation, La Jolla, CA 92037, USA.

*These authors contributed equally to this report.

†To whom correspondence should be addressed.